Origin of photocarrier traps in photorefractive α-$LiIO_3$ crystals by optical measurement and cluster calculation

Mamoru Kitaura*
Fukui National College of Technology, Sabae 916-8507, Japan

Naoyuki Fujita and Minoru Itoh
Department of Electrical and Electronic Engineering, Faculty of Engineering, Shinshu University, Nagano 380-8553, Japan

Hideyuki Nakagawa
Department of Electrical and Electronics Engineering, Faculty of Engineering, Fukui University, Fukui 910-8507, Japan
(Received 24 October 2005; revised manuscript received 25 January 2006; published 16 March 2006)

The electronic structure of α-$LiIO_3$ has been studied by the reflectivity and x-ray photoelectron experiments and by the discrete variational $X\alpha$ cluster calculation. The reflectivity spectrum exhibits a prominent peak at 5.56 eV near the fundamental edge. This peak is assigned to the $5s \rightarrow 5p$ intraionic transition of iodine. The main structures except the 5.56 eV peak are well explained in terms of the electronic transitions from the valence band composed of the O $2p$ state to the conduction band of the Li $2s$ state. The band gap locates at around 6.1 eV. The influence of Li imperfections on the electronic structure is also calculated for the model cluster. The result shows that photocarrier trap levels appear in the band gap. The formation of these trap levels is discussed in relation to the photorefractive effect in α-$LiIO_3$ crystals.

DOI: 10.1103/PhysRevB.73.115110 PACS number(s): 71.55.-i, 71.20.-b, 78.20.-e, 78.40.-q

I. INTRODUCTION

Lithium iodate crystallizes in two forms, hexagonal (α-type) and tetragonal (β-type), under normal conditions.[1,2] The crystal structure of α-$LiIO_3$ belongs to the space group $P6_3$. The lattice constants are $a=5.4815$ Å and $c=5.1709$ Å.[1] Schematic diagrams of the structure projected from the c and a axes are shown in Figs. 1(a) and 1(b), respectively. Two $LiIO_3$ molecules are included in the unit cell drawn by the broken line. Each iodine atom strongly bonds with three oxygen atoms to form an IO_3 molecule with C_3 symmetry. The IO_3 molecules are connected by Li atoms placed on the sixfold rotation axes.

Since α-$LiIO_3$ has a large electro-optic coefficient, it is expected to be a good candidate for photorefractive effects. Nevertheless, there are only a few studies on the photorefractive effect in pure and impurity-doped crystals.[3–5] It has been generally accepted that the photorefractive effect originates from trapping of photocreated electrons or holes at some deep levels in the band gap. Therefore, the formation of trap levels is of great importance, but there is no evidence for it in α-$LiIO_3$. On the other hand, this material is also known to be a quasi-one-dimensional ionic conductor.[6] From the experiments of anisotropic ionic conduction properties,[7–10] it has been suggested that there are two kinds of mobile ionic species. One is an interstitial Li ion which hops among interstices in a zigzag channel along the c axis, and the other is a Li vacancy which exchanges its position with Li ions at the regular lattice sites along the c axis. Thermal migration of Li ions is greatly enhanced by the superionic phase transition at the temperature $T=243$ K.[9] As pointed out in Ref. 5, this phenomenon has a close correlation with the weakening of photorefraction. It may be supposed that the formation of photocarrier trap levels due to interstitial Li ions and/or Li vacancies is responsible for the photorefractive effect in α-$LiIO_3$.

The purpose of the present study is to elucidate the influence of Li imperfections on the electronic structure of α-$LiIO_3$. No theoretical band calculation of this material has been reported. Optical studies are also limited to the energy region lower than the fundamental absorption edge.[10–12] It is therefore necessary to clarify the electronic structure of α-$LiIO_3$, as a first step. To do so, we have measured reflectivity and x-ray photoelectron spectra. The cluster calculation for the $[Li_7(IO_3)_{12}]^{-5}$ model cluster of Fig. 1(c) has been also performed using the discrete variational $X\alpha$ (DV-$X\alpha$) method. It is found that the result of cluster calculation is in good agreement with those of experiments. Next,

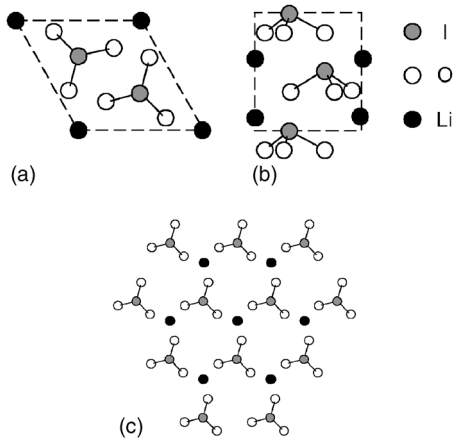

FIG. 1. (Color online) Schematic diagrams of the crystal structure of α-$LiIO_3$, projected in the direction of the c axis (a) and the a axis (b). The unit cell is indicated by a broken line. The structure of the $[Li_7(IO_3)_{12}]^{-5}$ model cluster (c) employed in this work.

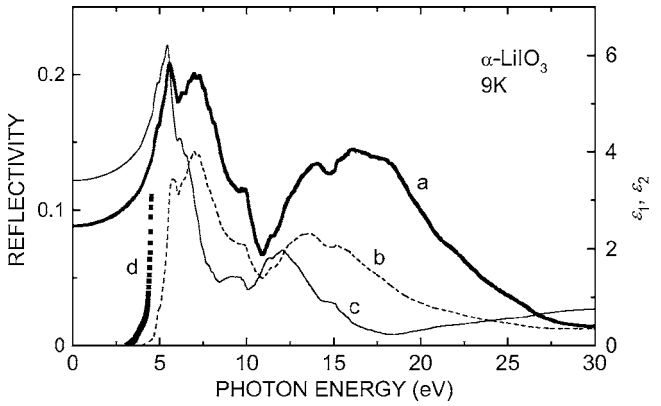

FIG. 2. The absorption edge spectrum (squares d) and reflectivity spectrum (thick solid line a) of α-$LiIO_3$ at 9 K. The real part ϵ_1 (thin solid line c) and the imaginary part ϵ_2 (broken line b) of the dielectric function derived by the Kramers-Kronig analysis.

the influence of an interstitial Li ion and a Li vacancy on the electronic structure is calculated for the model cluster. On the basis of these results, we discuss the photorefractive effect of α-$LiIO_3$ in connection to the formation mechanism of photocarrier trap levels.

II. EXPERIMENT

Stoichiometric quantities of regent-grade iodine pentoxide I_2O_5 and lithium carbonate Li_2CO_3 were dissolved in distilled water. The crystals of α-$LiIO_3$ were grown at room temperature by slow evaporation of the solution for nearly two months. They were transparent and have a hexagonal psuedo-prism shape with well-defined faces. The average dimension was $4\times2\times2$ mm^3.

The measurements of reflectivity spectra were carried out at the beamline BL7B of UVSOR facility at the Institute for Molecular Science, Okazaki. The synchrotron radiation was monochromatized by a 3-m normal incidence monochromator, the band pass being kept at 0.1 nm. The high-order light from the monochromator was eliminated by a quartz plate or a LiF crystal. The incident angle was about 15°. The incident and reflected light were detected by a calibrated silicon diode sensor (IRD AXUV-100). The base pressure in the sample chamber was 7.0×10^{-6} Pa during the experiment.

X-ray photoelectron spectroscopy (XPS) spectra were measured using an ESCA spectrometer (ULVAC-PHI 5600). Monochromatized x-ray source with an aluminium anode was used for excitation. An electron flood gun was employed to overcome sample charging under x-ray irradiation. The overall resolution was about 0.5 eV. The base pressure in the sample chamber was less than 6.0×10^{-8} Pa.

III. EXPERIMENTAL RESULTS

The absorption edge spectrum of α-$LiIO_3$ crystal at 9 K is shown by squares in Fig. 2. The absorption coefficient is rapidly increased at 4.3 eV, which corresponds to the fundamental absorption edge. On the low-energy side, an additional band is observed around 3.8 eV. This band is apparently of an extrinsic origin.

Generally speaking, it is very difficult to measure the absolute value of the reflectivity because of unavoidable light scattering at a crystal surface. The absolute reflectivity spectrum was obtained as follows. Since the refractive index n of α-$LiIO_3$ is available in the transparent region below 3.5 eV,[11] the absolute reflectivity $R(E)$ at photon energy E was calculated by substituting the values of $n(E)$ into the formula $R(E)=\{n(E)-1\}^2/\{n(E)+1\}^2$. The observed reflectivity spectrum was connected to the calculated one by multiplication with a constant factor. The reflectivity spectrum thus obtained is shown by a thick solid line in Fig. 2. This spectrum was measured for the polarization perpendicular to the crystallographic c axis. The reflectivity spectrum is composed of two parts: I (4–11 eV) and II (11–30 eV). In part I, three peaks are observed at 5.56, 7.07, and 9.92 eV. The lowest energy peak at 5.56 eV is relatively sharp, suggesting that it is of an excitonic origin. Part II is characterized by several broad bands.

From the reflectivity spectrum, the real part ϵ_1 and the imaginary part ϵ_2 of the complex dielectric constant were obtained by a Kramers-Kronig analysis. The spectra of ϵ_1 and ϵ_2 are shown by thin solid and broken lines in Fig. 2, respectively. The Kramers-Kronig analysis requires the reflectivity spectrum in the whole energy region from 0 to ∞. However, since our data is limited to the energy range of 3.5–30 eV, the values of reflectivity were extrapolated using the calculation ones below 3.5 eV and a function $R(E)=R(30\text{ eV})\cdot(30\text{ eV}/E)^p$ above 30 eV, where p is an adjustable parameter. Such an extrapolation of the $R(E)$ above 30 eV has been successfully adopted in semiconductors and insulators.[13] In these cases, the parameter p can be determined so that the value of ϵ_2 is zero at the fundamental absorption edge. The value of p thus obtained was 3.0. This value is smaller than 4.0, which is expected in sufficiently high-energy region. In the present study, the photon energy is not so high that the value of p should be smaller than 4.0. In fact, when $p=4$ was chosen, a spurious band appeared in the low-energy side of the fundamental absorption edge.

The spectra of ϵ_1 and ϵ_2 allow us the calculation of several optical constants; electron energy loss function $-\mathrm{Im}(1/\epsilon)$, effective number of electrons per molecule N_{eff}, and effective optical dielectric constant ϵ_∞. The values of N_{eff} and ϵ_∞ are given by the following fomulas, respectively:[14]

$$N_{\mathrm{eff}}=\frac{2m}{Nh^2e^2}\int_0^E\frac{\epsilon_2(E')}{E'}dE', \tag{3.1}$$

$$\epsilon_\infty=1+\frac{2}{\pi}\int_0^E\frac{\epsilon_2(E')}{E'}dE', \tag{3.2}$$

where N is the number of molecules per unit volume, m and e are the mass and charge of an electron, respectively, and h is the Planck constant. The spectra of $-\mathrm{Im}(1/\epsilon)$, N_{eff}, and ϵ_∞ are shown in Figs. 3(a)–3(c), respectively. In Fig. 3(a), several loss peaks are observed in the 5–15 eV range. An intense band around 21 eV is probably due to the bulk plasmon

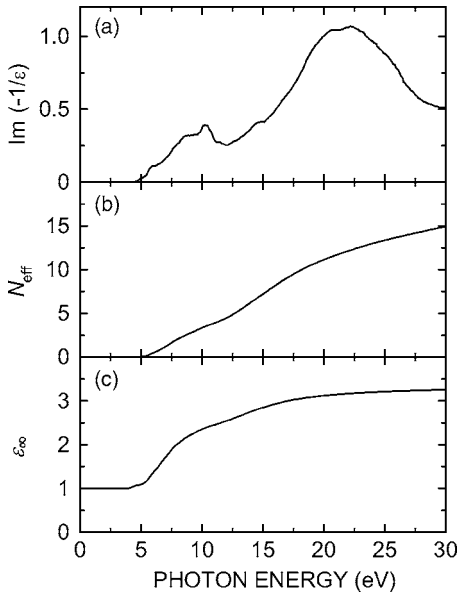

FIG. 3. Optical spectra of α-$LiIO_3$: (a) electron energy loss function $-\mathrm{Im}(1/\epsilon)$, (b) effective number of electrons per molecule N_{eff}, and (c) effective optical dielectric constant ϵ_∞.

formation. The value of N_{eff} in Fig. 3(b) monotonuously increases with photon energy. The increase in N_{eff} is weakly suppressed at around 18 eV. The value of ϵ_∞ in Fig. 3(c) rapidly increases in the range of 5–15 eV and reaches 3.25 at 30 eV.

Figure 4(a) shows the XPS spectrum of α-$LiIO_3$ crystal at room temperature. The binding energy is given relative to the top of the valence band (VB). The XPS spectrum consists of four peaks at 3.3, 6.5, 12.3, and 20.4 eV. The 20.4 eV peak is broader than the other three, suggesting that it is composed of at least two subbands.

IV. DV-$X\alpha$ CALCULATION

In order to investigate the electronic structure of α-$LiIO_3$ theoretically, we carried out nonrelativistic molecular orbital calculations by the DV-$X\alpha$ cluster method. This method has been successfully applied to the analysis of a variety of functions in organic and inorganic compounds. The methodological details are described in Ref. 15. The $[Li_7(IO_3)_{12}]^{-5}$ model cluster was used in our calculation, which was shown in Fig. 1(c). The point symmetry of this cluster is C_3. The coordinations of ions were determined by referring to Ref. 1. The basic functions used were 1s to 2p orbitals for Li, 1s to 5p for I, and 1s to 2p for O. The influence of the Madelung potential due to all ions outside the cluster was taken into account.

Figure 4(b) presents the partial density-of-states (PDOS) curves that were obtained by assuming that each energy level has a Gaussian shape with a full width at half maximum of 0.5 eV. The energy is given relative to the top of the VB. The VB is mainly composed of the O 2p states, and partially of the I 5s and 5p states. The outermost core state at −9.49 eV corresponds to an admixture of the I 5s, O 2s, and O 2p states. The doublet due to the O 2s state locates at −17.88 and −20.38 eV. On the other hand, the bottom of the conduction band (CB) is mainly formed by the I 5p states, with some contributions from the Li 2s and Li 2p, and O 2p states. In the higher-lying CB, two PDOS peaks are seen at 10.93 and 14.59 eV. They are predominantly constituted of the Li 2s and 2p states. The band gap is calculated to be 6.15 eV.

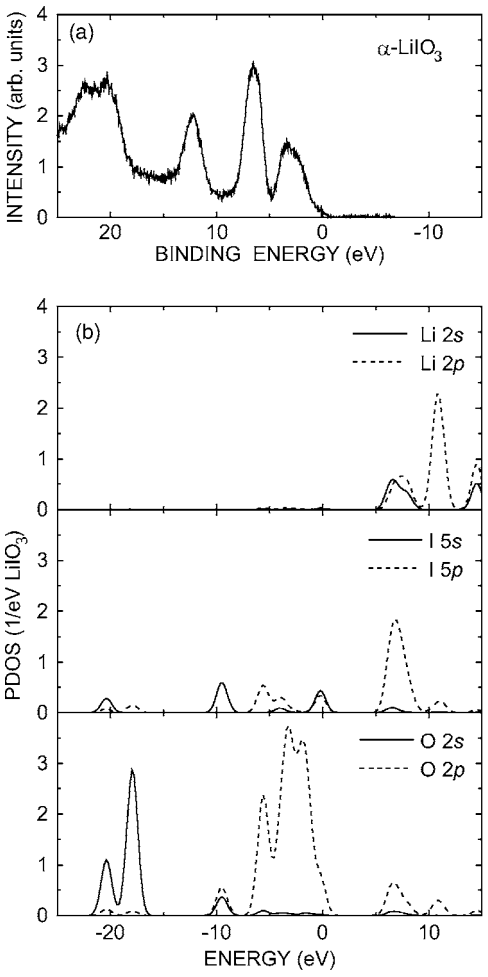

FIG. 4. (a) XPS spectrum of α-$LiIO_3$ excited by Al K_α line. The binding energy is given relative to the top of the VB. (b) Partial density-of-states (PDOS) per molecule calculated for the $[Li_7(IO_3)_{12}]^{5-}$ model cluster of Fig. 1(c). The energy distribution curves of PDOS are shown for the electronic orbitals of Li, I, and O. The top of the VB is taken as zero energy.

V. DISCUSSION OF OPTICAL PROPERTIES

At the beginning, we shall discuss the optical properties of α-$LiIO_3$ by reference to the electronic structure obtained from the DV-$X\alpha$ calculation. As shown in Fig. 4(a), the XPS spectrum exhibits four bands at 3.3, 6.5, 12.3, and 20.4 eV. The 3.3 and 6.5 eV bands are assigned to the upper and lower VB, respectively. According to the PDOS curves of Fig. 4(b), the upper VB is composed of two peaks at −1.80 and −3.20 eV, and the lower VB of a single peak at −5.60 eV. This feature is compatible with the fact that the 3.3 eV band is relatively broad as compared with the 6.5 eV

band. The outermost core band at 12.3 eV is ascribed to the bonding state of I 5*s*, O 2*s*, and O 2*p*, since its position is close to the −9.40 eV band in the PDOS curve. A broad band around 20.4 eV is composed of, at least, two subbands. Since the PDOS curve due to O 2*s* exhibits a double structure, the 20.4 eV band is likely assigned to the O 2*s* state. This is supported by the fact that the O 2*s* peak is seen at around 20 eV in XPS spectra of some metal oxides.[16]

The reflectivity spectrum consists of two parts, I (4–11 eV) and II (11–30 eV), as shown by a thick solid line in Fig. 2. These two parts are most likely caused by the electronic transitions from the O 2*p* valence states. The electronic transitions are basically parity allowed for the final states with *s* character. The PDOS curves show that the Li 2*s* states contribute to the lower and upper CB. Therefore, the O $2p \rightarrow$ Li 2*s* transitions are most plausible for the origin of the main structures in I and II. It is to be noted that the $5s \rightarrow 5p$ transition at cationic iodine ions is also possible in part I. This type of transition is observed as a sharp peak near the fundamantal edge of the absorption spectrum, as seen in lead compounds.[17] In fact, a prominent peak is observed at 5.56 eV in Fig. 3. This peak would be connected to the formation of cationic excitons at iodine sites.

From the reflectivity spectrum of Fig. 2, the band gap is supposed to locate at around 6.1 eV. On the other hand, the band gap energy is estimated as 6.15 eV by the DV-$X\alpha$ calculation. The agreement between experiment and calculation is very good, revealing that the model cluster of $[Li_7(IO_3)_{12}]^{-5}$ is suitable for the description of the energy level structure of α-$LiIO_3$. This is an important result of our study. If the cluster size is small, the band gap energy is not correctly reproduced in the DV-$X\alpha$ calculation.[18]

As shown in Fig. 3(b), N_{eff} reaches 10 around 18 eV, which corresponds to the onset of the transition from the I 5*s* outermost core level to the I 5*p* lower CB. The value of 10 is smaller than the number of valence electrons per molecule estimated from the sum of the 2*p* electrons of three O ions and the 5*s* electrons of one I ion. This result seems to be acceptable, because it satisfies the general rule that the value of N_{eff} does not exceed the number of valence electrons in the energy region below the transition from an outermost core level.[14] From Fig. 3(c), it appears that ϵ_∞ reaches a saturation value 3.25 with increasing photon energy. The value of 3.25 is close to the optical dielectric constant (3.4095) estimated from the dispersion formula.[11] It is thus evident that the main contribution to the optical dielectric constant comes from ϵ_2 in the energy region below 30 eV; in other words, an extrapolation of $R(E)$ above 30 eV does not significantly affect the results of the Kramers-Kronig analysis.

VI. ORIGIN OF PHOTOREFRACTIVE EFFECT

As mentioned in Sec. I, it is supposed that the existense of interstitial Li ions and/or Li vacancies is essential for manifestation of the photorefractive effect in α-$LiIO_3$. The electronic states associated with Li imperfections are of great interest. We therefore calculated the electronic structures for two kinds of clusters, $[Li_6(IO_3)_{12}]^{-5}$ and $[Li_8(IO_3)_{12}]^{-5}$. The

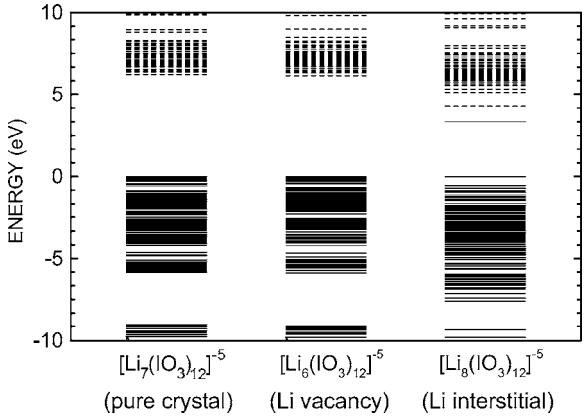

FIG. 5. Energy level diagrams of $[Li_6(IO_3)_{12}]^{-5}$ and $[Li_8(IO_3)_{12}]^{-5}$ clusters. For referenece, the energy level diagram of $[Li_7(IO_3)_{12}]^{-5}$ cluster is depicted on the left-hand side. The top of the VB is taken as zero energy. The occupied and unoccupied levels are represented by solid and broken straight lines, respectively.

former and latter contain a Li vacancy at the center and an interstitial Li ion at an interstitial site, respectively. The position of interstitial Li ion was determined by referring to Ref. 7. The charges of +1 and −1 were given to the whole of the former and latter clusters, respectively, to maintain the electrical neutrality of the crystal lattice. These given charges appear as a hole bound to a Li vacancy and an electron to an interstitial Li ion, respectively. The energy level diagrams of $[Li_6(IO_3)_{12}]^{-5}$ and $[Li_8(IO_3)_{12}]^{-5}$ are shown in Fig. 5, where the energy level of $[Li_7(IO_3)_{12}]^{-5}$ is also presented for comparison. Solid and broken lines represent occupied and unoccupied levels, respectively. The overall energy level structure is not influenced by the introduction of a Li vacancy, except for the appearance of an accepterlike level above the VB by 47 meV. On the contrary, the introduction of an interstitial Li ion causes some remarkable changes in the energy level structure: (i) decrease of the band gap energy, (ii) widening of the VB, and (iii) appearance of donorlike levels below the CB by 0.83 and 1.77 eV. From an analysis of the bond overlap population, it turns out that these levels originate in the formation of an antibonding between I and O ions and a bonding between interstitial Li and nearest neighbor I ions.

In Ref. 5, the activation energy for thermal quenching of photorefraction is reported to be 0.32 eV, in agreement with that for migration of Li ions. The depth energy 47 meV of the acceptorlike level in $[Li_6(IO_3)_{12}]^{-5}$ is too small compared with 0.32 eV. This suggests that the Li vacancy is not responsible for the photorefractive effect. On the other hand, the depth of the donorlike levels in $[Li_8(IO_3)_{12}]^{-5}$ is deep enough. We therefore suppose that the interstitial Li ion is the most plausible candidate for the origin of the photorefraction. From a two-wave mixing experiment,[5] Xu *et al.* found that dominant charge carriers in α-$LiIO_3$ are electrons. Because interstitial Li ions form donorlike levels, photocreated electrons have a chance to be trapped by them.

In the crystal lattice of α-$LiIO_3$, an interstitial Li ion couples with the nearest neighbor I ion and the surrounding O ions. As a result, a number of localized levels appear in the

band gap. In our calculation, an analysis of the bond overlap population reveals that these levels are mainly of antibonding character for I–O and partially of bonding character for Li–I, as mentioned above. When an electron occupies one of these levels, the I–O bond is remarkably weakened, whereas the Li–I bond is reinforced. It is supposed that the trapping of electrons by the donorlike levels is ascribed to a strengthening of the Li–I bond around an interstitial Li ion.

It is known that the trapping of both electrons and holes takes place in the initial stage of the photorefractive effect. No information on trapped holes in α-$LiIO_3$ is found in literature. In the present study, we focused our attention on the influence of Li imperfections on the electronic structure, and found that the hole trap levels due to Li vacancies are not responsible for the photorefractive effect. However, this does not mean the nonexistence of trapped holes in α-$LiIO_3$. As seen from the PDOS curves in Fig. 4(b), the contribution of the O $2p$ orbital is dominant on the top of the VB. Since a large part of valence holes distribute on the oxygen orbital, it is expected that they are self-trapped at oxygen sites. Such self-trapping of valence holes is a common feature in metal oxides.[19] Therefore, it is reasonably suggested that self-trapped holes are formed in α-$LiIO_3$, and play an essential role for the photorefractive effect, in cooperation with electrons trapped at interstitial Li ions.

VII. SUMMARY

In the present study, we have measured the reflectivity and x-ray photoelectron spectra of α-$LiIO_3$. These spectra are compared with the electronic structure calculated by the DV-$X\alpha$ method. From the reflectivity spectrum, we get the band gap energy to be 6.1 eV, in good agreement with the calculated one. The entire spectrum above the band gap is ascribed to the electronic transitions from the VB composed of O $2p$ to the CB of Li $2s$. The Kramers-Kronig analysis is carried out to obtain some optical constants. The structures in XPS spectrum are consistent with the calculated PDOS curves. These results indicate that the model cluster adopted by us is quite suitable.

From our calculation, it is revealed that the introduction of an interstitial Li ion forms some electron trap levels in the band gap. The present study shows no clear indication of trapped holes. The valence holes are probably self-trapped on oxygen ions, as in the case of other oxides. These trapped electrons and holes are suggested to be a key factor for the photorefractive effect in α-$LiIO_3$. Further experimental studies such as transient absorption and EPR are required to clarify the nature of trap centers.

ACKNOWLEDGMENTS

We are grateful to M. Kawabata for his assistance in the experiment. One of us (M.K.) acknowledges the financial support by a Grant-in-Aid from the Ministry of Education, Culture, Sport, Science, and Technology of Japan. The present work was partly carried out at the UVSOR facility under the Joint Studies Program of the Institute for Molecular Science.

*E-mail address: kitaura@fukui-nct.ac.jp

[1] A. Rosenzweig and B. Morosin, Acta Crystallogr. **20**, 758 (1966).
[2] J. Liebertz, Z. Phys. Chem., Neue Folge **67**, 94 (1969).
[3] A. R. Pogosyan, E. M. Urykin, and G. F. Dobrzhanskii, Sov. Phys. Solid State **24**, 2063 (1982).
[4] F. Laeri, R. Jumgen, G. Angelows, U. Vietze, T. Engel, M. Wurzt, and D. Hilgenberg, Appl. Phys. B: Lasers Opt. **54**, 351 (1995).
[5] J. Xu, X. Yue, and R. A. Rupp, Phys. Rev. B **54**, 16618 (1996).
[6] S. Haussuhl, Phys. Status Solidi **29**, K159 (1968).
[7] T. C. Li and Z. Y. Xu, Acta Phys. Sin. **26**, 500 (1977).
[8] A. D. Zhang, S. F. Zhao, A. Y. Xie, and Z. Y. Xu, Acta Phys. Sin. **29**, 1158 (1980).
[9] A. E. Aliev, A. Sh. Akramov, L. N. Fershtat, and P. K. Khabibullaev, Phys. Status Solidi A **108**, 189 (1988).
[10] M. A. Gaffar and A. A. El. Fadl, J. Phys. Chem. Solids **60**, 1633 (1999).
[11] K. Takizawa, M. Okada, and S. Ieiri, Opt. Commun. **23**, 279 (1977).
[12] K. Koralewski and M. Szatranski, J. Mol. Struct. **142**, 139 (1986).
[13] F. Wooten, *Optical Properties of Solids* (Academic, New York, 1972).
[14] H. R. Philipp and E. Ehrenreich, Phys. Rev. **131**, 2016 (1963).
[15] H. Adachi, M. Tsukada, and C. Satoko, J. Phys. Soc. Jpn. **45**, 875 (1978).
[16] J. F. Moulder, W. F. Stickle, P. E. Sobol, and K. D. Bomben, *Handbook of X-Ray Photoelectron Spectroscopy*, edited by J. Chastain (Perkin-Elmer Coorporation, Eden, Ptairie, MN, 1992).
[17] M. Fujita, M. Itoh, Y. Bokumoto, H. Nakagawa, D. L. Alov, and M. Kitaura, Phys. Rev. B **61**, 15731 (2000).
[18] I. Tanaka, M. Mizuno, and H. Adachi, Phys. Rev. B **56**, 3536 (1997).
[19] N. Itoh and A. M. Stoneham, *Materials Modification by Electronic Excitation* (Cambridge University Press, Cambridge, 2001).